Search for Supersymmetry in Events with one Photon, Jets and missing transverse Energy at $\sqrt{s} = 8$ TeV

Maximilian Knut Kiesel on behalf of the CMS collaboration

1. Physikalisches Institut B, RWTH Aachen University, Aachen, Germany

DOI: http://dx.doi.org/10.3204/DESY-PROC-2014-04/278

Gauge mediated supersymmetry breaking (GMSB) [1] is a scenario for physics beyond the standard model (SM) which can stabilize the mass of the SM Higgs boson, allow the grand unification of forces, and avoid the flavor problems endemic in other SUSY breaking scenarios.

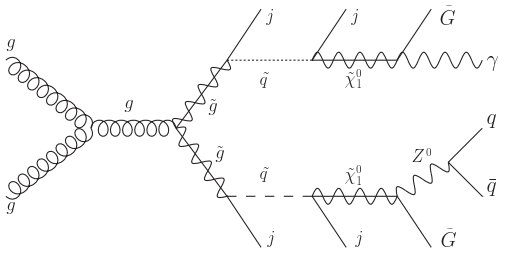

Figure 1: Event diagram for a typical photon final state expected within the GGM framework for a wino-like neutralino. A gluino pair is produced, which decays via squarks to neutralinos. The neutralinos decay to a photon or Z boson and a gravitino.

This search [2] is interpreted in the context of General Gauge Mediation (GGM) [3], in which the lightest SUSY particle is the gravitino ($\tilde{G}$) and the next-to-lightest SUSY particle the lightest neutralino ($\tilde{\chi}_1^0$), which can decay to a photon and a $\tilde{G}$ if the $\tilde{\chi}_1^0$ is bino- or wino-like. A typical process is shown in Fig. 1. R-parity is assumed to be conserved.

The data was recorded with the CMS detector [4] at the LHC during the 2012 run period with a center-of-mass energy of $\sqrt{s} = 8\,\text{TeV}$. It corresponds to an integrated luminosity of $19.7\,\text{fb}^{-1}$. On trigger level, one photon candidate with large transverse momentum and hadronic activity is required.

For the signal region, events with at least one photon reconstructed in the central part of the detector and with a transvere momentum $p_{\text{T}^*} \geq 110\,\text{GeV}$, hadronic activity $H_{\text{T}} \geq 500\,\text{GeV}$, two jets, missing transverse energy $\not{E}_{\text{T}} \geq 100\,\text{GeV}$, but no electrons nor muons are selected. The $\not{E}_{\text{T}}$ and the particles which are clustered to jets are reconstructed using the particle-flow (PF) algorithm. The H_{T} is the scalar sum of the transverse momentum of all jets and all photon-like objects. The transverse momentum of the photon (p_{T^*}) is not estimaded by the energy deposit in the electromagnetic calorimeter only, but is estimated by the $p_{\text{T}}$of the matched jet to the photon. This measurement of the transverse momentum is compatible for real photons and jets with a large neutral electromagnetic component. This is important for the major background estimation method, which relies on a similar kinematic for both types of objects. In addition, the photon identification requires that the energy deposits in the calorimeters must be photon-like. To discriminate between electrons and photons, the activity in in the

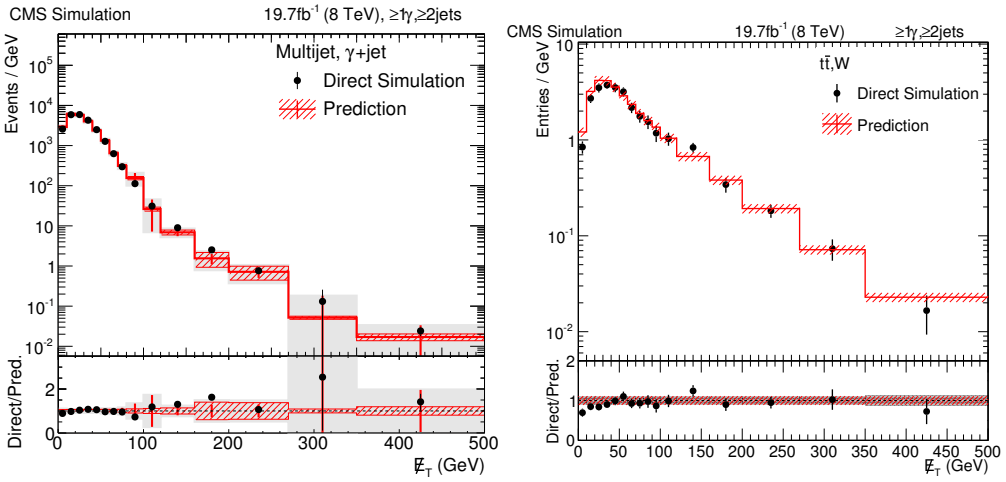

Figure 2: $\not\!\!E_{\mathrm{T}}$ distribution for simulated multijet and photon plus jet events (left) and simulated $\mathrm{t\bar{t}}$ and W boson events (right). The hatched area shows the systematical uncertainty of the data-driven background estimation method, and the gray area the total uncertainty.

tracker between vertex and the energy deposit in the calorimeter is restricted. Photons are also required to be isolated from other particles. Therefore, the sums of p_T of all charged hadrons, neutral hadrons and photons (except for the photon candidate itself), reconstructed with the PF algorithm within $\Delta R < 0.3$ to the photon candidate are calculated. These isolation deposits from charged hadrons ($\mathrm{I}_{\pm}$), neutral hadrons (I_0), and photons (I_γ) are required to be smaller than a threshold depending on the photon's transverse momentum.

The dominant background from SM processes origins from photon plus jet, or multijet events where one jet is misidentified as a photon. Mismeasurement of jets can lead to large $\not\!\!E_{\mathrm{T}}$ in these events. The contribution of these events to the signal region is estimated simultaneously from events with photon-like jets and low missing transverse energy using data. The photon-like jets are similar to the photon with respect to the shower shape, the tracker activity and the hadronic component, but have larger isolation deposits $\mathrm{I}_{\pm}$, I_0, and I_γ. The ratio of the number of events in the signal region to the number of events in this control region is calculated for $\not\!\!E_{\mathrm{T}} < 100\,\mathrm{GeV}$ in bins of $p_{\mathrm{T}*}$ and the hadronic recoil. Hadronic recoil is the vectorial sum of the p_T of all jets, excluding the photon(-like) object. Events of the control sample with $\not\!\!E_{\mathrm{T}} \geq 100\,\mathrm{GeV}$ are scaled by this weight to estimate the contribution of multijet and photon plus jet production in the signal region. This method is tested on simulation: Figure 2 (left) shows the $\not\!\!E_{\mathrm{T}}$ distribution for simulated multijet and photon plus jet events compared to the prediction by the method described above. The direct simulation is in agreement with the prediction from simulation.

The contribution from electrons being misidentified as photons is estimated also from data. The probability of an electron faking a photon ($f_{e\to\gamma}$) is measured using the tag-and-probe method with $Z \to ee$ events. The rate is evaluated in bins of p_{T}, number of tracks emerging from the Z-boson vertex, and the number of vertices. A multidimensional fit is used to parametrize the misidentification probability. To estimate the background, a control region with electrons is defined by selecting photon candidates with hits in the tracker, which can be extrapolated to the energy deposit in the calorimeter. This sample is scaled event-by-event by $f_{e\to\gamma}$. Figure 2 (right)

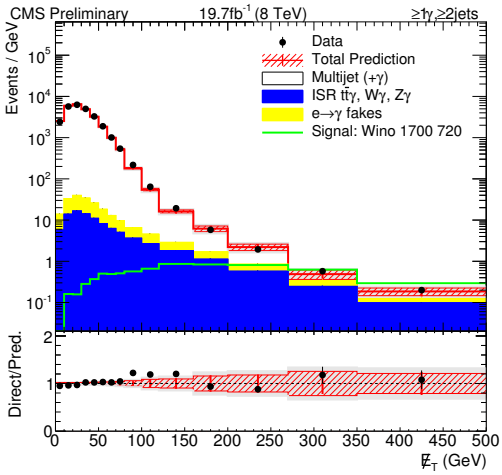

Figure 3: Total standard model background prediction as a function of $\not\!\!E_{\mathrm{T}}$ compared to data. In addition GGM signal benchmark point with a wino-like neutralino with a neutralino mass of 375 GeV, a squark mass of 1700 GeV, and a gluino mass of 720 GeV is shown. The bottom ratio plot shows the event yields relative to the total background prediction. The hatched area represents the systematic uncertainty, the error bars the statistic uncertainty and the gray band the total uncertainty.

shows the $\not\!\!E_{\mathrm{T}}$ distribution for simulated $\mathrm{t\bar{t}}$ and W boson events compared to the prediction by the method described above. The direct simulation is in agreement with the prediction from simulation. Especially for high $\not\!\!E_{\mathrm{T}}$, initial and final state radiation (ISR/FSR) contribute to the signal region. MADGRAPH [5] is used to simulate $\mathrm{t\bar{t}}\gamma$, $\mathrm{W}\gamma$, and $\mathrm{Z}\gamma \to \nu\nu\gamma$ processes, which are scaled by a common scale factor. This scale factor is estimated by comparing MCFN [6] calculations, cross-section measurements and verification in a control region with $\mathrm{Z}\gamma \to \mu\mu\gamma$ events. Events with electrons or muons are rejected in order to reduce the contribution from events with initial and final state radiation.

Figure 3 shows the total SM background prediction and the signal selection as function of $\not\!\!E_{\mathrm{T}}$. A signal benchmark point with a $\tilde{\chi}_1^0$ mass of 375 GeV, a squark mass of 1700 GeV, and a gluino mass of 720 GeV is drawn in addition. The data is in agreement with the SM background prediction. The event yields, the background composition and the yields for the same signal benchmark point is shown in Table 1 for the bins used in the statistical interpretation. The result is interpreted in the GGM framework for bino- or wino-like neutralino scenarios as function of squark and gluino masses. The $\tilde{\chi}_1^0$ mass (and in the wino-like neutralino scenario the lightest chargino mass) is set to 375 GeV. Multi-channel counting experiments in the six distinct $\not\!\!E_{\mathrm{T}}$-bins shown in Table 1 are combined into a single limit. The $\mathrm{CL_s}$ method is used to determine exclusions at 95% confidence level. Possible contamination of signal in the control sample used for background estimation is found to be of the order of 5–40%, and is considered in the limit calculation. Figure 4 shows the observed cross section limit (left) and the corresponding exclusion contours (right) for a wino-like neutralino scenario. For the bino-like neutralino scenario, gluino (squark) masses of 1100 (1350) GeV are excluded.

$\not{E}_T$ Range [GeV]	[100, 120)	[120, 160)	[160, 200)	[200, 270)	[270, 350)	[350, ∞)
Multijet(+photon)	991±164	529±114	180±69	95.6±45	11.7±12	9.1±9
Electron	37.3±4	42.5±5	23.0±3	19.2±2	7.7±1.0	4.1±0.6
ISR/FSR	53.6±27	72.5±36	44.9±23	40.1±20	19.7±10	14.7±7
Background	1082±166	644±119	248±73	155±50	39.0±16	27.8±12
Data	1286	774	232	136	46	30
Signal	18.8±3	53.1±5	50.5±5	82.3±7	77.7±7	67.3±6
Backg. from signal	2.1	5.0	5.6	9.9	26.7	13.5
Acceptance [%]	0.3	0.9	0.8	1.3	1.2	1.1
Exp. limit [pb]	5.23	1.21	0.57	0.24	0.14	0.11
Obs. limit [pb]	6.03	1.89	0.55	0.21	0.18	0.11

Table 1: Resulting event yields, estimated background, and yields for a GGM signal scenario for a wino-like neutralino scenario with a neutralino mass of 375 GeV, a squark mass of 1700 GeV, a gluino mass of 720 GeV, and a cross section of 316 fb. The combined observed (expected) CLs cross-section limit for this point is 99 fb (91 fb) at 95% CL.

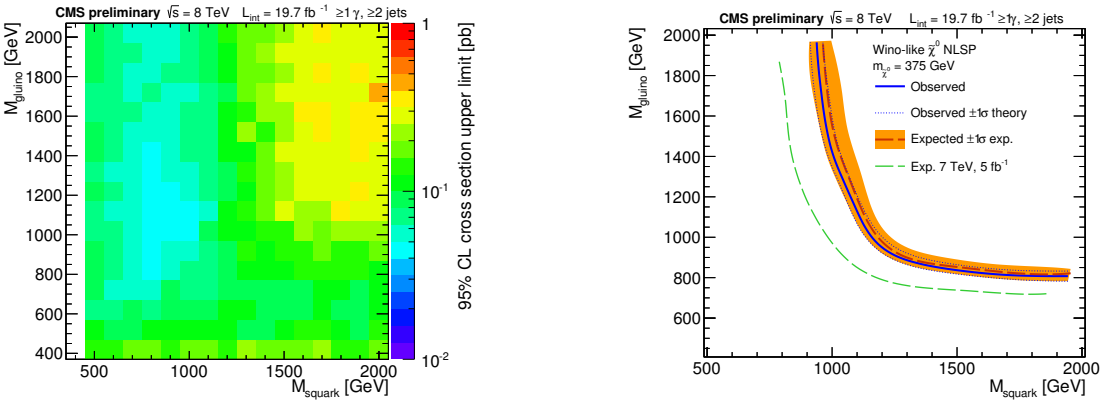

Figure 4: Observed upper limits (left) and exclusion contours (right) at 95% C.L. on the signal cross section in the gluino-squark mass space for the wino-like neutralino scenario. The exclusion contour of the previous analysis [7] is drawn in addition.

References

[1] Pierre Fayet. Mixing Between Gravitational and Weak Interactions Through the Massive Gravitino. *Phys.Lett.*, B70:461, 1977.

[2] CMS Collaboration. Search for supersymmetry in events with one photon, jets and missing transverse energy at $\sqrt{s} = 8$ TeV. CMS-PAS-SUS-14-004. 2014.

[3] Patrick Meade, Nathan Seiberg, and David Shih. General Gauge Mediation. *Prog.Theor.Phys.Suppl.*, 177:143–158, 2009.

[4] S. Chatrchyan et al. The CMS experiment at the CERN LHC. *JINST*, 3:S08004, 2008.

[5] Johan Alwall, Michel Herquet, Fabio Maltoni, Olivier Mattelaer, and Tim Stelzer. MadGraph 5 : Going Beyond. *JHEP*, 1106:128, 2011.

[6] John M. Campbell, Heribertus B. Hartanto, and Ciaran Williams. Next-to-leading order predictions for $Z\gamma$+jet and Z $\gamma\gamma$ final states at the LHC. *JHEP*, 1211:162, 2012.

[7] Serguei Chatrchyan et al. Search for new physics in events with photons, jets, and missing transverse energy in pp collisions at $\sqrt{s} = 7$ TeV. *JHEP*, 1303:111, 2013.